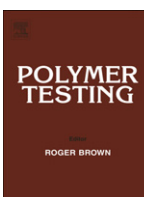




ELSEVIER

Contents lists available at ScienceDirect

Polymer Testing

journal homepage: www.elsevier.com/locate/polytest

Property modelling

Mechanical behavior of polytetrafluoroethylene in tensile loading under different strain rates

L.C.S. Nunes*, F.W.R. Dias, H.S. da Costa Mattos

Laboratory of Theoretical and Applied Mechanics, LMTA, Graduate Program of Mechanical Engineering, PGMEC, Universidade Federal Fluminense, UFF, Rua Passo da Patria 156, 24210-240 Niterói, RJ, Brazil

ARTICLE INFO

Article history:

Received 10 June 2011

Accepted 22 July 2011

Keywords:

Polytetrafluoroethylene

Strain rates

Constitutive model

ABSTRACT

The present work is concerned with the study of the mechanical behavior of polytetrafluoroethylene (PTFE) in tensile tests performed under different strain rates using standard specimens. The strains are measured through a non-contact video extensometer. This procedure is particularly accurate since large deformations are involved. A mathematical model is proposed to predict the mechanical behavior observed in the experiments. The main goal is to predict the stress-strain curve under different strain rates using model equations that combine enough mathematical simplicity to allow their use in engineering problems with the capability of describing complex non-linear mechanical behaviour. The material constants that appear in the model equations can be easily identified from only three tests performed at different constant strain rates. Results from experimental tensile testing were compared with the model predictions showing a good agreement.

© 2011 Elsevier Ltd. Open access under the [Elsevier OA license](http://creativecommons.org/licenses/by/3.0/).

1. Introduction

In recent years polytetrafluoroethylene (PTFE) has received considerable attention due to its special physical characteristics such as high melting point, very good resistance against chemicals and extremely low friction. The complex nonlinear behaviour of polytetrafluoroethylene remains one of the most severe limitations for its even wider use in the chemical and petrochemical industries. PTFE specimens have been tested in compression and tension at differing strain rates and temperatures [1,2]. Experimental tests of relaxation in tension of PTFE were developed and the results compared with the prediction of Maxwell's model [3]. Ratcheting behavior of PTFE has been investigated at room and elevated temperatures [4,5]. A single specimen normalization technique was employed to evaluate the J-integral fracture toughness of PTFE for a range of temperatures and loading rates [6]. Several constitutive models have been proposed to predict the complex mechanical behavior of thermoplastic and thermoset materials. Strain rate and

temperature-dependent behavior of polymers has been described by means of constitutive models [7–13]. Also, some studies were made to report deformation damage in solid polymers [14–17]. The mechanical behavior of polymers under high strain rates has been presented in the literature [18–20]. Mechanical characterization of PTFE using a non-contact and full-field optical method has been proposed [21].

The combined effect of rate dependency and very large inelastic deformations can be extremely complex. The mechanisms proposed so far to explain microscopically the material behavior are not able to elucidate all aspects of these coupled phenomena. In a certain sense, the material behavior of PTFE can be considered superplastic. A wide class of materials - metals, ceramics, intermetallics, nanocrystalline, polymer, etc - show superplastic behavior under special processing conditions. The most important characteristic of a superplastic material is its high strain rate sensitivity of flow stress that confers a high resistance to neck development and results in the high tensile elongations characteristic of superplastic behavior. Superplastically deformed material in tensile tests gets thinner in a very uniform manner, rather than forming a 'neck' (a local narrowing), which leads to fracture [22].

* Corresponding author. Tel./fax: +55 21 2629 5588.

E-mail address: luzcsn@mec.uff.br (L.C.S. Nunes).

Although, up to now, there is no precise physical definition of superplasticity phenomenon in polymeric materials; from a phenomenological point of view, superplasticity can be defined as very high deformations prior to local failure. In the case of tensile tests under controlled strain rate, this means very high elongations of the specimens before rupture. Despite the lack of definition of any fundamental mechanism for superplastic behavior, the evaluation of the influence of strain rate on superplastic properties of a polymer sheet material is a basic requirement for its economical use. This objective is accomplished by the execution of a set of tensile tests at different rates.

The purpose of this work is to propose a mathematical model for describing mechanical behavior of PTFE in tensile loading under different strain rates. The (large) strain measures obtained using a non-contact video extensometer are used as input to the control system of the testing machine. A theoretical model is proposed that is based on classical saturation and power law models. The main goal is to predict the stress-strain curve under different strain rates using model equations that combine enough mathematical simplicity to allow their use in engineering problems with the capability of describing complex non-linear mechanical behavior. Also, the experimental identification of the parameters that appear in the model must be as simple as possible. The material constants that appear in the model equations can be easily identified from only three tests performed at different constant strain rates. It is interesting to note that these model equations can be obtained within a thermodynamic context similar to that done by Costa Mattos et al. in [23–25] for different kinds of structure under tensile loading. The main contribution of this work is to present a simple but reliable alternative approach to predict the mechanical behavior of PTFE at different strain rates.

It is also important to note that the present study is mainly focused on the influence of the strain rate on the material response in tensile tests performed at room temperature and it is not the goal to discuss the microscopic mechanisms involved.

2. Experimental

2.1. Material

The material used in this investigation is a commercially available PTFE (DuPont Teflon[®]), which is characterized by a density of $2.18 \times 10^3 \text{ kg/m}^3$ and a melting temperature about 327°C .

The standard tension test specimens were manufactured from PTFE with shape and size specified by ASTM D-638-08 (Type I) [26]. The initial gage length l_0 and initial cross section A_0 are, respectively, 50 mm and 26 mm^2 ($13 \text{ mm} \times 2 \text{ mm}$) as illustrated in Fig. 1.

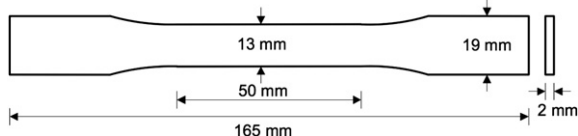


Fig. 1. Standard tension test specimen dimensions.

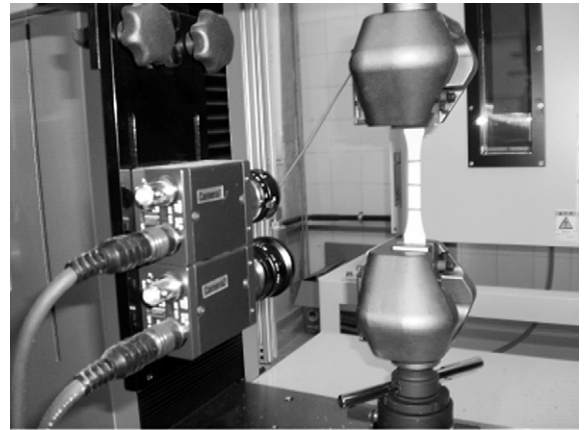


Fig. 2. Experimental non-contact arrangement.

2.2. Tensile test procedure

Tensile tests were performed using an electro-mechanical Shimadzu AG-X universal testing machine. The gauge length elongation of PTFE specimens was measured using an optical method. The experimental non-contact method is based on two CCD cameras, as illustrated in Fig. 2. The video extensometers produce a real time image of the useful portion of the specimen, which is used to measure the elongation of the gauge length. It is important to emphasize that all experiments were carried out at room temperature, i.e., 25°C . The engineering strain rates (6.0×10^{-4} , 7.7×10^{-2} , 9.2×10^{-2} and $1.3 \times 10^{-1} \text{ s}^{-1}$, see next section) were controlled by using the measured elongation as input to the control system of the testing machine.

3. Results and discussion

3.1. True and engineering relationship definitions

Using prescribed elongation $\Delta l(t)$ and applied force $F(t)$ experimentally measured, in addition to the initial gage length l_0 and initial cross section A_0 , the engineering strain ϵ and the engineering stress s are given by

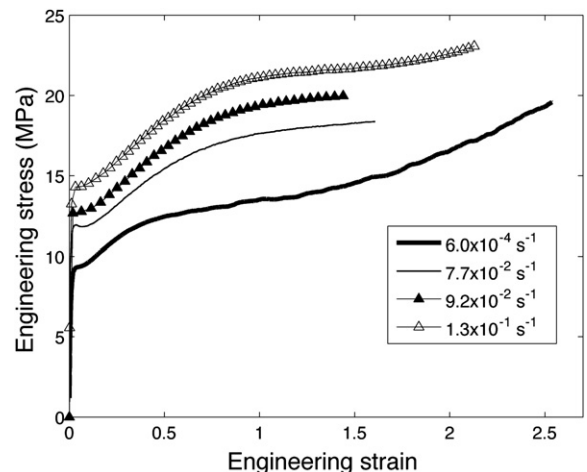


Fig. 3. Engineering stress-strain curve.

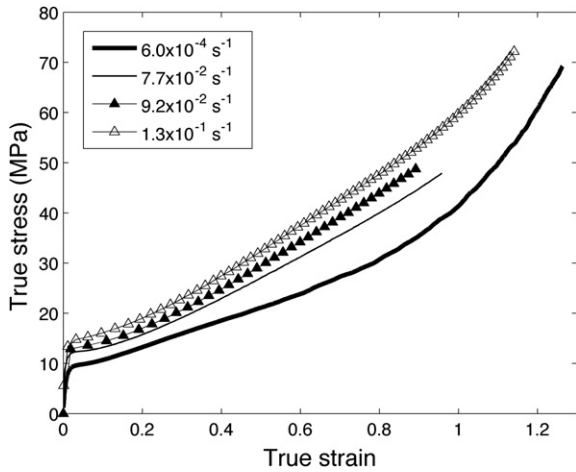


Fig. 4. True stress-strain curve.

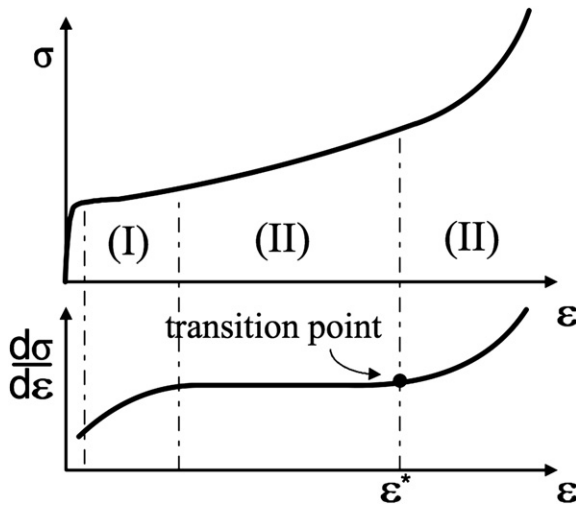


Fig. 5. Schematic representation of stress-strain and slope curves: definition of ϵ^* .

$$e(t) = \frac{\Delta l(t)}{l_0} \text{ and } s(t) = \frac{F(t)}{A_0} \quad (1)$$

With constant volume, the true strain and true stress as a function of e and s are defined as

$$\epsilon = \ln(1 + e) \text{ and } \sigma = s(1 + e) \quad (2)$$

Figs. 3 and 4 illustrate engineering and true stress-strain curves of PTFE for different constant engineering strain rates: $\dot{\epsilon}_1 = 6.0 \times 10^{-4}$, $\dot{\epsilon}_2 = 7.7 \times 10^{-2}$, $\dot{\epsilon}_3 = 9.2 \times 10^{-2}$, $\dot{\epsilon}_4 = 1.3 \times 10^{-1} \text{ s}^{-1}$. These results were obtained from experimental data using Eqs. (1) and (2). The curves show a strong strain rate dependency, in which the flow stress increases with strain rate.

Disregarding the small strain region ($\epsilon < 4\%$), for all cases, the true stress-strain curve has three distinct regions: (i) region I, initially $\partial^2\sigma/\partial\epsilon^2$ is high, however it gradually decreases; (ii) region II, where $\partial^2\sigma/\partial\epsilon^2$ tends to zero and (iii) region III, $\partial^2\sigma/\partial\epsilon^2$ increases again (see Fig. 5). Fig. 5 illustrates a schematic representation of the true stress-strain curve and the slope of this curve, in which ϵ^* is defined as the strain value associated with the transition between region II and region III. Experimentally, it is observed that ϵ^* is not very sensitive to the strain rate and, thus, it can be assumed as a material constant.

One of the characteristics of PTFE is to present large deformations under tension prior to local failure. Fig. 6 illustrates a sequence of images of a typical PTFE specimen under monotonic loading until failure. Specimen deformation is very homogeneous. The high strain rate sensitivity of flow stress confers a high resistance to neck development: the specimen gets thinner in a very uniform manner, rather than forming a 'neck'. In general, failure is localized and characterized by a crack perpendicular to the tensile axis.

3.2. Modeling

In this section, a phenomenological constitutive model for polytetrafluoroethylene in tensile loading is introduced. The proposed mathematical model is divided into two parts: the first part is defined by a true strain range varying

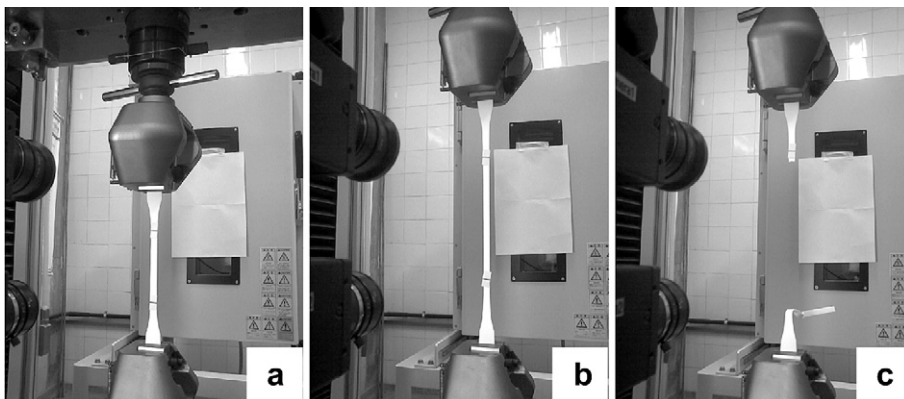


Fig. 6. Large deformations observation of the PTFE specimen under tensile loads.

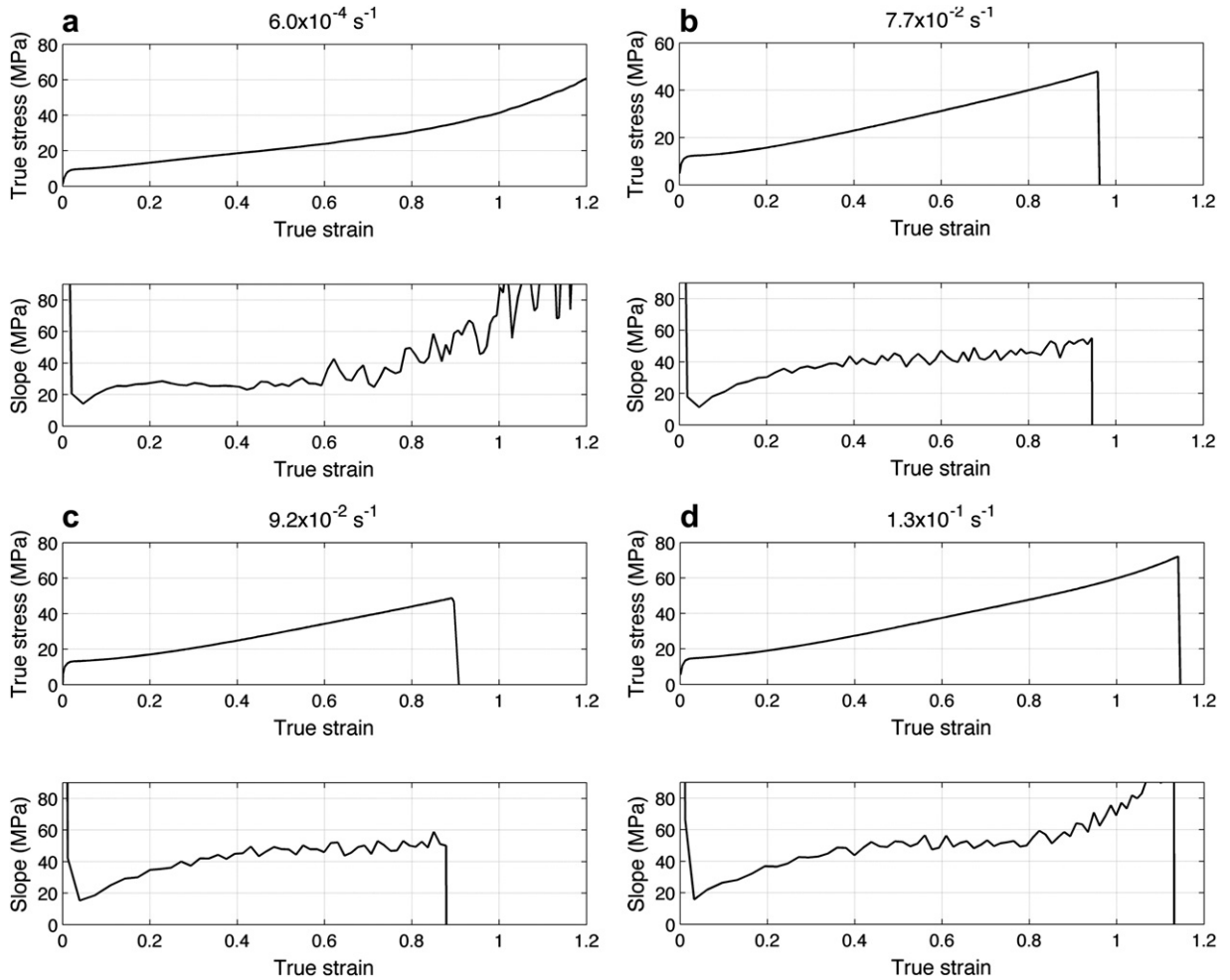


Fig. 7. True stress-strain curves and slope for different engineering strain rates: (a) $6.0 \times 10^{-4} \text{ s}^{-1}$, (b) $7.7 \times 10^{-2} \text{ s}^{-1}$, (c) $9.2 \times 10^{-2} \text{ s}^{-1}$ and (d) $1.3 \times 10^{-1} \text{ s}^{-1}$.

from 0 to ε^* , while the second one is taken for true strain value larger than ε^* .

In order to find an adequate expression to model the mechanical behavior of PTFE under tensile loading performed at different strain rates, the following mathematical model is proposed,

$$\sigma = \begin{cases} \sigma_f(\varepsilon, \dot{\varepsilon})\{[1 - \exp(-\beta\varepsilon)] + K_I\varepsilon^n\} & 0 < \varepsilon \leq \varepsilon^* \\ \sigma_f^* + K_{II}(\varepsilon - \varepsilon^*)^m, & \varepsilon > \varepsilon^* \end{cases} \quad (3)$$

The first part of the mathematical model proposed is based on a saturation model, where β is defined as a positive material constant. The rate dependency is described

through the flow stress σ_f , which is supposed to be given by the following expression:

$$\sigma_f(\dot{\varepsilon}, \varepsilon) = A\dot{\varepsilon}\exp(\varepsilon) + B \quad (4)$$

where A and B are constants to be determined.

In addition to this expression, a power law is considered with strength coefficient and strain-hardening exponent K_I and n , respectively. It is important to note that K_I and n are assumed to be associated with stretch of non-orientated molecular chains. The second part of the mathematical modeling proposed is defined by the strength coefficient K_{II} and the strain-hardening exponent m , in this case these

Table 1

Results of first part for strain values less than ε^* .

Engineering strain-rate $\dot{\varepsilon}(\text{s}^{-1})$	σ_f (MPa)	β	K_I (MPa)	n
6×10^{-4}	9.6	160	2.83	1.247
7.7×10^{-2}	12.38	320.8	3.056	1.427
9.2×10^{-2}	12.88	542.9	3.223	1.403
1.3×10^{-1}	14.78	243.2	3.018	1.413

Table 2

Results of second part for strain values large than ε^* .

Engineering strain-rate $\dot{\varepsilon}(\text{s}^{-1})$	σ_f^* (MPa)	K_{II} (MPa)	m
6×10^{-4}	30.74	110.9	1.4
7.7×10^{-2}	40.07		
9.2×10^{-2}	44		
1.3×10^{-1}	47.84		

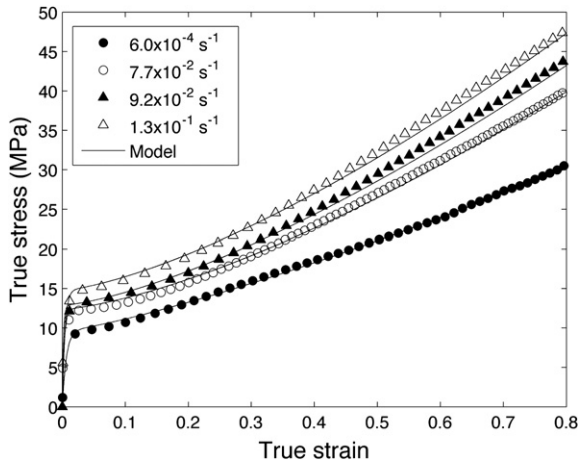


Fig. 8. Experimental and model true stress-strain curve for different strain rates: $(0 < \epsilon \leq \epsilon^*)$.

two parameters are related to oriented molecular chains. By definition, $\sigma_f^* = \sigma(\epsilon^*)$.

3.3. Parameters identification

As mentioned in the previous section, the proposed model (see Eq. (3)), can be divided into two parts, where the parameter ϵ^* must be determined first. For estimating this parameter, the last transition point (transition between region II and III) from the slope of true stress-strain curve was taken into account. Fig. 7(a–d) show the experimental data of true stress-strain curves and the relative slopes for different constant engineering strain rates. The value of ϵ^* is assumed approximately equal to 0.8 for all cases. Note that in Fig. 7(b) and (c), the rupture occurs immediately after this value.

The next step is to estimate the parameters: σ_f, β, K_I and n from the first part of Eq. (3) and σ_f^*, K_{II} and m from the second part for each engineering strain rate. In order to do this, all parameters were estimated using the Levenberg–Marquardt method [27–29], which is a well-known and powerful iterative method for solving

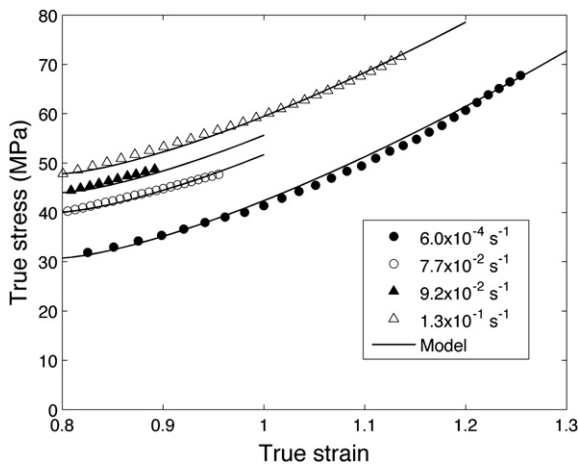


Fig. 9. Experimental and model true stress-strain curve for different strain rates: $\epsilon > \epsilon^*$

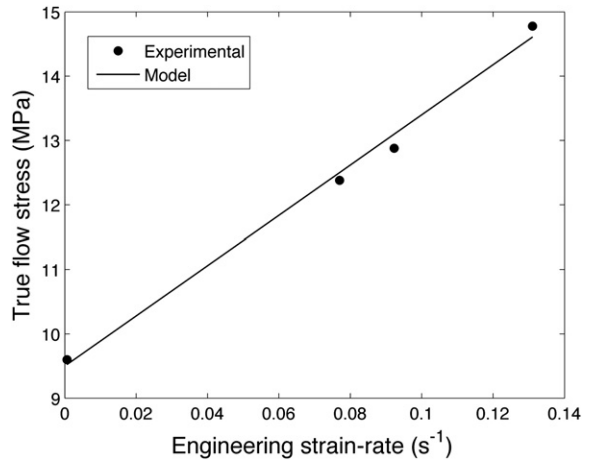


Fig. 10. True flow stress as a function of engineering strain rate.

nonlinear least squares problems of parameter estimation. These parameters, for different engineering strain rates, are displayed in Tables 1 and 2.

Experimental data and the proposed model considering all estimated parameters are plotted in Figs. 8 and 9. However, it is suggested for practical purposes to consider β, K_I and n as material constants. For this reason, it is suggested to consider the mean values of these parameters, i.e. $\beta_m = 317, K_{Im} = 3.12 \text{MPa}, n = 1.4$.

The rate dependency is included in the modeling through σ_f and using Eq. (4). It is important to observe that, from Eq (2), the relation between engineering and true strain rates is given by

$$\dot{\epsilon} = \frac{\dot{\epsilon}}{1 + e} = \frac{\dot{\epsilon}}{\exp(\epsilon)} \text{ or } \dot{\epsilon} = \dot{\epsilon} \exp(\epsilon) \tag{5}$$

Therefore, Eq. (4) can be rewritten in the form

$$\sigma(\dot{\epsilon}, \epsilon) = \sigma(\dot{\epsilon}) = A\dot{\epsilon} + B \tag{6}$$

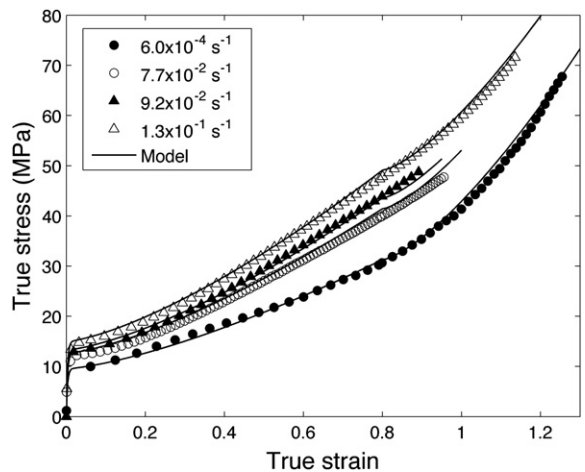


Fig. 11. Experimental and adjusted model true stress-strain curve for different strain rates.

Fig. 10 illustrates both experimental data and model prediction, where it is found that $A = 39$ MPas and $B = 9.5$ MPa.

3.4. Validation

In order to validate the proposed model, the experimental data are compared with model predictions considering $\beta_m = 317$, $K_{lm} = 3.12$ MPa, $n = 1.4$, $A = 39$ MPas and $B = 9.5$ MPa. Four different strain rates are considered: $\dot{\epsilon}_1 = 6.0 \times 10^{-4}$, $\dot{\epsilon}_2 = 7.7 \times 10^{-2}$, $\dot{\epsilon}_3 = 9.2 \times 10^{-2}$, $\dot{\epsilon}_4 = 1.3 \times 10^{-1} s^{-1}$.

Clearly, from the results shown in Fig. 11, good agreement can be seen between experimental data and the proposed model using estimated parameters. The small discrepancy can be attributed to material response, which is very complex. Moreover, it is important to emphasize that with only three tests, considering three different strain rates, are sufficient to predict the mechanical behavior of the PTFE.

4. Conclusions

The strain rate dependency of polytetrafluoroethylene (PTFE) specimens in tensile tests was analyzed. The large deformations were measured using a non-contact optical extensometer. Monotonic tests performed under controlled engineering strain rates were performed. An alternative mathematical model was proposed for predicting the mechanical behavior. It is interesting to note that these model equations can be obtained within a thermodynamic context in a similar manner to that done by Costa Mattos et al. in [22–25] for different mechanical applications. The proposed model assumes that the material response can be split into two parts. Only three tests performed with different controlled strain rates are necessary to identify all material constants that appear in the theory. The main goal is to use the model to obtain the maximum information about the macroscopic properties of polytetrafluoroethylene specimens in tensile tests performed at room temperature with different strain rates from a minimum set of laboratory tests, saving time and reducing experimental costs.

Acknowledgements

The financial support of Rio de Janeiro State Funding, FAPERJ, and Research and Teaching National Council, CNPq, are gratefully and acknowledged.

References

- [1] P.J. Rae, D.M. Dattelbaum, The properties of poly(tetrafluoroethylene) (PTFE) in compression, *Polymer* 45 (2004) 7615–7625.
- [2] P.J. Rae, E.N. Brown, The properties of poly(tetrafluoroethylene) (PTFE) in tension, *Polymer* 46 (2005) 8128–8140.
- [3] A. Hernández-Jiménez, J. Hernández-Santiago, A. Macías-García, J. Sánchez-González, Relaxation modulus in PMMA and PTFE fitting by fractional Maxwell model, *Polym. Test* 21 (2002) 325–331.
- [4] Z. Zhang, X. Chen, Y. Wang, Uniaxial ratcheting behavior of polytetrafluoroethylene at elevated temperature, *Polym. Test.* 29 (2010) 352–357.
- [5] Z. Zhang, X. Chen, Multiaxial ratcheting behavior of PTFE at room temperature, *Polym. Test.* 28 (2009) 288–295.
- [6] E.N. Brown, D.M. Dattelbaum, The role of crystalline phase on fracture and microstructure evolution of polytetrafluoroethylene (PTFE), *Polymer* 46 (2005) 3056–3068.
- [7] C. Ebert, W. Hufenbach, A. Langkamp, M. Gude, Modelling of strain rate dependent deformation behaviour of polypropylene, *Polym. Test.* 30 (2011) 183–187.
- [8] J. Richeton, S. Ahzi, K.S. Vecchio, F.C. Jiang, R.R. Adharapurapu, Influence of temperature and strain rate on the mechanical behavior of three amorphous polymers: characterization and modeling of the compressive yield stress, *Int. J. Solids Struct.* 43 (2006) 2318–2335.
- [9] B. Farrokh, A.S. Khan, A strain rate dependent yield criterion for isotropic polymers: low to high rates of loading, *Euro J. Mech. A/ Solids* 29 (2010) 274–282.
- [10] Erhard Krempf, Fazeel Khan, Rate (time)-dependent deformation behavior: an overview of some properties of metals and solid polymers, *Int. J. Plasticity* 19 (2003) 1069–1095.
- [11] Qin-Zhi Fang, T.J. Wang, H.G. Beom, H.P. Zhao, Rate-dependent large deformation behavior of PC/ABS, *Polymer* 50 (2009) 296–304.
- [12] M. Wendlandt, T.A. Tervoort, U.W. Suter, Non-linear, rate-dependent strain-hardening behavior of polymer glasses, *Polymer* 46 (2005) 11786–11797.
- [13] J.S. Bergstrom, L.B. Hilbert Jr., A constitutive model for predicting the large deformation thermomechanical behavior of fluoropolymers, *Mech. Mater.* 37 (2005) 899–913.
- [14] C.Y. Tang, C.P. Tsui, W. Shen, C.C. Li, L.H. Peng, Modelling of non-linear stress-strain behaviour of HIPS with craze damage in tensile loading-unloading process, *Polym. Test.* 20 (2001) 15–28.
- [15] F. Za'ri, M. Na't-Abdelaziz, J.M. Glogaen, J.M. Lefebvre, Modelling of the elasto-viscoplastic damage behaviour of glassy polymers, *Int. J. Plasticity* 24 (2008) 945–965.
- [16] C. C'Sell, J.M. Hiver, A. Dahoun, Experimental characterization of deformation damage in solid polymers under tension, and its interrelation with necking, *Int. J. Solids Struct.* 39 (2002) 3857–3872.
- [17] E.N. Brown, P.J. Rae, E.B. Orlor, The influence of temperature and strain rate on the constitutive and damage responses of polychlorotrifluoroethylene (PCTFE, Kel-F 81), *Polymer* 47 (2006) 7506–7518.
- [18] N.K. Naik, Y. Perla, Mechanical behaviour of acrylic under high strain rate tensile loading, *Polym. Test.* 27 (2008) 504–512.
- [19] M. Schoßg, C. Bieröel, W. Grellmann, Thomas Mecklenburg, Mechanical behavior of glass-fiber reinforced thermoplastic materials under high strain rates, *Polym. Test.* 27 (2008) 893–900.
- [20] A.D. Mulliken, M.C. Boyce, Mechanics of the rate-dependent elastic-plastic deformation of glassy polymers from low to high strain rates, *Int. J. Solids Struct.* 43 (2006) 1331–1356.
- [21] L.C.S. Nunes, Mechanical characterization of polytetrafluoroethylene polymer using full-field displacement method, *Opt. Lasers Eng.* 49 (2011) 640–646.
- [22] H.S. da Costa Mattos, G. Minak, F. Di Gioacchino, A. Soldà, Modeling the superplastic behavior of Mg alloy sheets under tension using a continuum damage theory, *Mater. Design* 30 (2009) 1674–1679.
- [23] H.S. da Costa Mattos, I.N. Bastos, J.A.C.P. Gomes, A simple model for slow strain rate and constant load corrosion tests of austenitic stainless steel in acid aqueous solution containing sodium chloride, *Corros. Sci.* 50 (2008) 2858–2866.
- [24] H.S. da Costa Mattos, A.H. Monteiro, E.M. Sampaio, Modelling the strength of bonded butt-joints, *Compos. B. Eng.* 41 (2010) 654–662.
- [25] H.S. da Costa-Mattos, F.E.G. Chimisso, Modelling creep tests in HMPE fibres used in ultra-deep-sea mooring ropes, *Int. J. Solids Struct.* 48 (2011) 144–152.
- [26] Standard test method for tensile properties of plastics. ASTM – D 638–08.
- [27] K. Levenberg, A method for the solution of certain problems in least squares, *Quart. Appl. Math.* 2 (1944) 164–168.
- [28] D. Marquardt, An Algorithm for least-squares Estimation of nonlinear parameters, *SIAM J. Appl. Math.* 11 (1963) 431–441.
- [29] P.R. Gill, W. Murray, M.H. Wright, "The Levenberg-Marquardt Method." §4.7.3 in *Practical Optimization*. Academic Press, London, 1981, 136–137.